# EMULATE Deliverable D11: Assessment of time varying influence of SST and atmospheric circulation on European surface temperature and precipitation.


## Hadley Centre (Partner 2), UEA (Partner 1), UA (Partner 3), CEA (Partner 4), URV (Partner 5), UBERN (Partner 6), SU (Stockholm University)

Tara Ansell[1], Chris Folland[1], David Fereday[1], Adam Scaife[1], Jeff Knight[1], Andreas Philipp[2], Jucundus Jacobeit[2], Paul Della-Marta[3], Pascal Yiou[4], Nicolas Fauchereau[4], David Lister[5], Phil Jones[5], Anders Moberg[6], Rezwan Mohammad[6], Manola Brunet[7].

[1] – Hadley Centre, Met Office, UK
[2] – University of Augsburg, Germany
[3] – University of Bern, Switzerland
[4] – CEA, France
[5] – CRU, UEA, UK
[6] – Stockholm University, Sweden
[7] – Universitat Rovira i Virgili, Spain


## 1) Introduction

Winter temperatures and precipitation amounts in Europe are known to be quite strongly influenced by the North Atlantic Oscillation (NAO) and may also be affected by other circulation and sea-surface temperature (SST) patterns. Summer precipitation totals in Europe as a whole are less influenced by the summer NAO (though the UK is an exception) but show marked multi decadal variability and are related to global-scale SST and atmospheric circulation variability. Such observed links have important implications for predictability. So a clear goal of EMULATE has been to document these relationships, using new and extended datasets of daily pressure, temperature and precipitation, in addition to the existing, high quality SST analysis, HadISST [Rayner *et al.,* 2003].

We document here the *observed* seasonal relationships between the atmospheric variables (pressure, temperature, precipitation) and SST. Similar work was presented in D7 (extended in D12 and D13) using GCM *simulations*. The relationships between the observed variables over the last 150 years in all seasons will be examined and the temporal stability of the relationships will be assessed, with an emphasis on whether late-20$^{th}$ century patterns differ from patterns in the 19$^{th}$ Century.

This work is based on the cluster patterns of Philipp *et al.* [2006] (WP2 deliverable 5) and Fereday *et al*. [2006], using the EMSLP daily fields [Ansell *et al.*, 2006] (WP1 deliverable 3). We consider firstly the stationarity of these cluster patterns through the 19$^{th}$ and 20$^{th}$ century (section 2). We then look at the lead-lag relationships between these patterns with local and global SST (section 3). The relationship between these characteristic circulation patterns and European temperature and precipitation is addressed in section 4, with a focus on extreme events and time varying influence. We then extend this analysis of extremes to focus on European droughts in section 5. We take a more global perspective and consider the impact of ENSO in section 6. Finally, in section 7, we examine links between atmospheric circulation and the Ratcliffe and Murray (RM) North Atlantic SST pattern in winter. Concluding remarks are given in section 8.

## 2) Assess stationarity of clusters between 19th and 20th Century

As part of WP2 (presented in Philipp *et al.* [2006]) characteristic atmospheric circulation patterns for each season were defined using the EMSLP data set [Ansell *et al.* 2006]. The degree of stationarity of these cluster patterns was assessed by comparing the daily MSLP clustering between the whole EMULATE period (1850-2003) with three different sub periods (SP1: 1850-1900, SP2: 1901-1951, SP3: 1952-2003). A high degree of stationarity would be present if all principal patterns of a particular season were identified in all sub periods, with only minor variations in frequency or in shape of the patterns. Substantial non-stationarity would be indicated if merging or splitting of particular patterns could be observed for some of the sub periods.

Our analysis indicated distinct seasonal differences in the degree of non stationarity with maxima during the transition seasons and low levels for summer and winter. For winter (Figure 1), all principal patterns were clearly identified during all sub periods, though there were some noteworthy changes in rankings, indicating either circulation changes from the 19th-20th century or different data quality and reconstruction skills. During summer (Figure 2) all the principal patterns from the whole period were clearly identified during all the sub periods, with only minor changes in frequency.

For spring (MAM) the degree of stationarity is much lower, with only a few cluster patterns being recognised in all sub periods. This may partly be due to the higher number of clusters, implying a higher probability for changes between different sub periods. It may also be indicative of the larger variability during this transitional season. For autumn (SON) complete correspondence for all patterns was only achieved within the 20th century (i.e. between SP2 and SP3). The SON and MAM plots are available from http://phygeo7.geo.uni-augsburg.de/emulate/wp3/ .

## 3) Observed links with SST

A number of previous works e.g. Ratcliffe and Murray [1970]; Palmer and Sun [1985]; Lau and Nath [1990]; Rodwell et al [1999] and Rodwell and Folland [2002, 2003] have found links between SST and North Atlantic-European circulation patterns. More recently Moron and Plaut [2003] and Cassou *et al.* [2004] used cluster patterns to explore SST-circulation links. Here we report on recent findings of Fereday et al [2006], drawing also on Philipp *et al.* [2006]. We are even more sure now of the long-term accuracy and homogeneity of the Hadley Centre SST data that has been used due to the tests recently published in Folland (2005).

In Figure 3, global SSTs are regressed on the two month season JF cluster 1 (positive phase of NAO) frequency time series, revealing the well documented SST tripole pattern. The link between the NAO cluster and SSTs is apparent when the SSTs lead by one month, but become stronger when SSTs lag by one month (Figure 3, lower RHS panel).

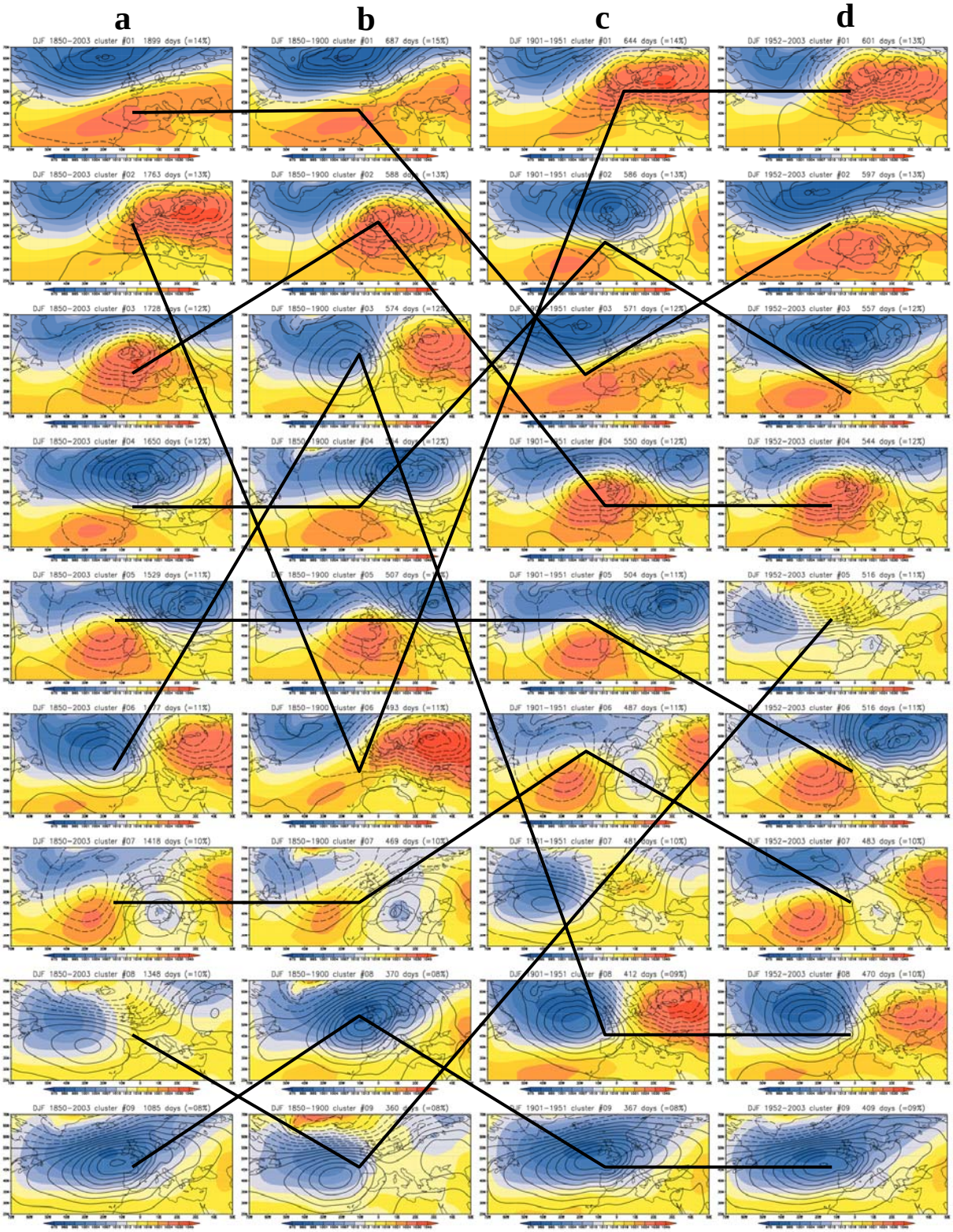


**Figure 1**: EMSLP clusters for winter (DJF) ranked according to their relative frequency of occurrence (highest frequency at the top). The diagrams show sea level pressure and their anomalies (interval 2hPa, dashed is positive)) determined for column a) 1850-2003 and separately for various sub-periods: column b) 1850-1900, column c) 1901-1951 and column d) 1952-2003. Connecting black lines denote a close similarity in the shape of given clusters between the different periods.

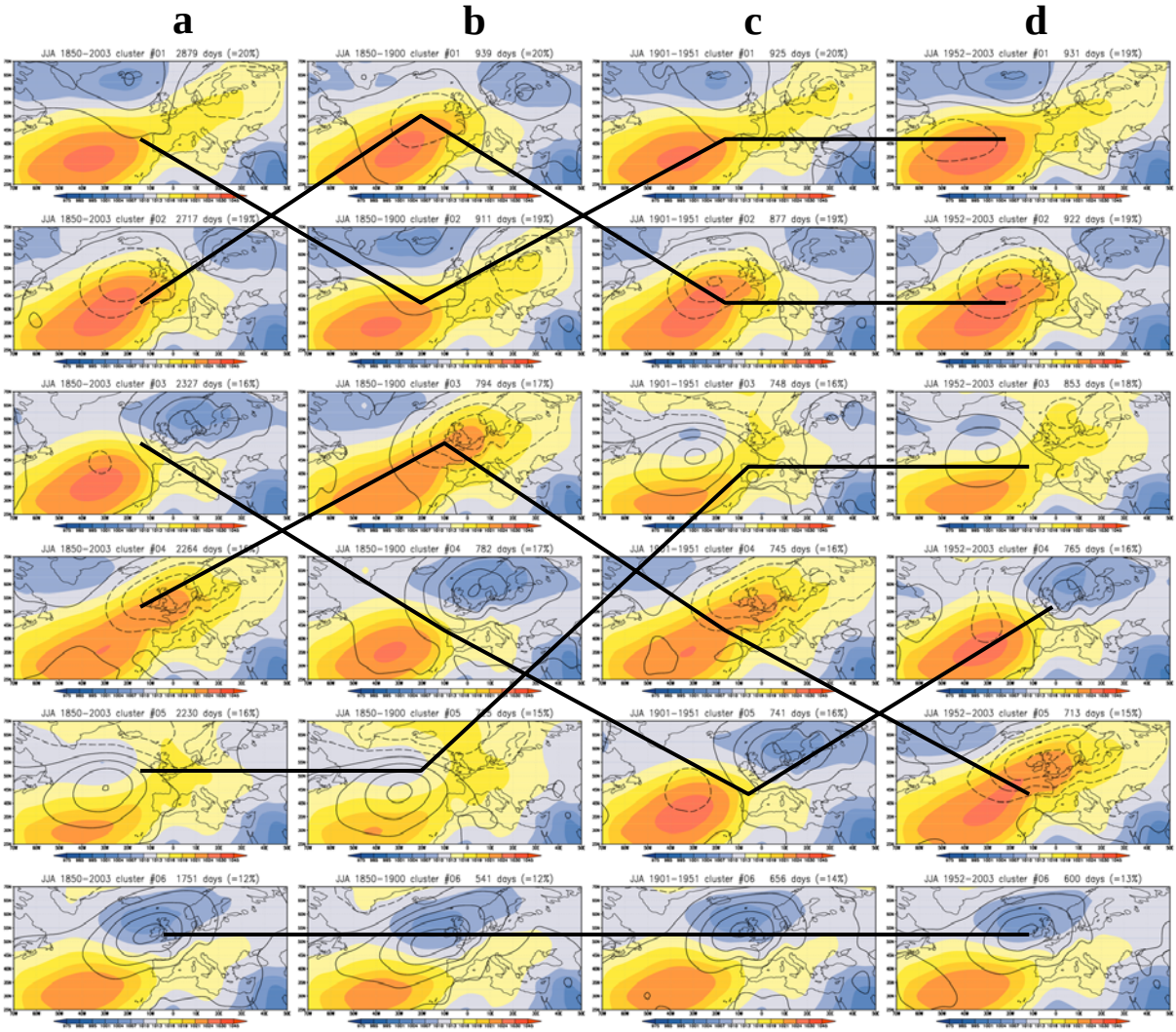


**Figure 2**: EMSLP clusters for summer (JJA) ranked according to their relative frequency of occurrence (highest frequency at the top). The diagrams show sea level pressure and their anomalies (interval 2hPa, dashed is positive)) determined for column a) 1850-2003 and separately for various sub-periods: column b) 1850-1900, column c) 1901-1951 and column d) 1952-2003. Connecting black lines denote a close similarity in the shape of given clusters between the different periods.

In the JA (high summer) season, the dominant mode of atmospheric variability for the North Atlantic-European region is the summer equivalent of the winter NAO, the summer NAO [SNAO, Hurrell & Folland, 2002], accounting for at least 20% of the variance in JA. Two JA clusters (4 and 6 (similar to JJA cluster 4 in Figure 2)) were identified as opposite phases of the SNAO pattern. A time series of the SNAO was produced by subtracting the negative phase's frequency time series from that of the positive phase. Regression of these series shows different SST associations at different time scales (Figure 4). On multidecadal time scales, a broad global pattern with predominantly cold SSTs in the Northern Hemisphere and warm SSTs in the Southern Hemisphere is seen, strongly resembling the negative phase of the Atlantic Multidecadal Oscillation (AMO) [Knight *et al.*, 2005]. This suggests multidecadal modulation of the SNAO. In contrast, the interannual relationship shows a prominent El Niño pattern, with high SST anomalies across the equatorial Pacific, indicating a link between UK and European summer climate with tropical Pacific variability hitherto unseen in the literature [Fereday *et al.* 2006]. This may be indicative of some potential interannual predictability in this season. Some further detail of the links between the SNAO and ENSO is given in section 6.

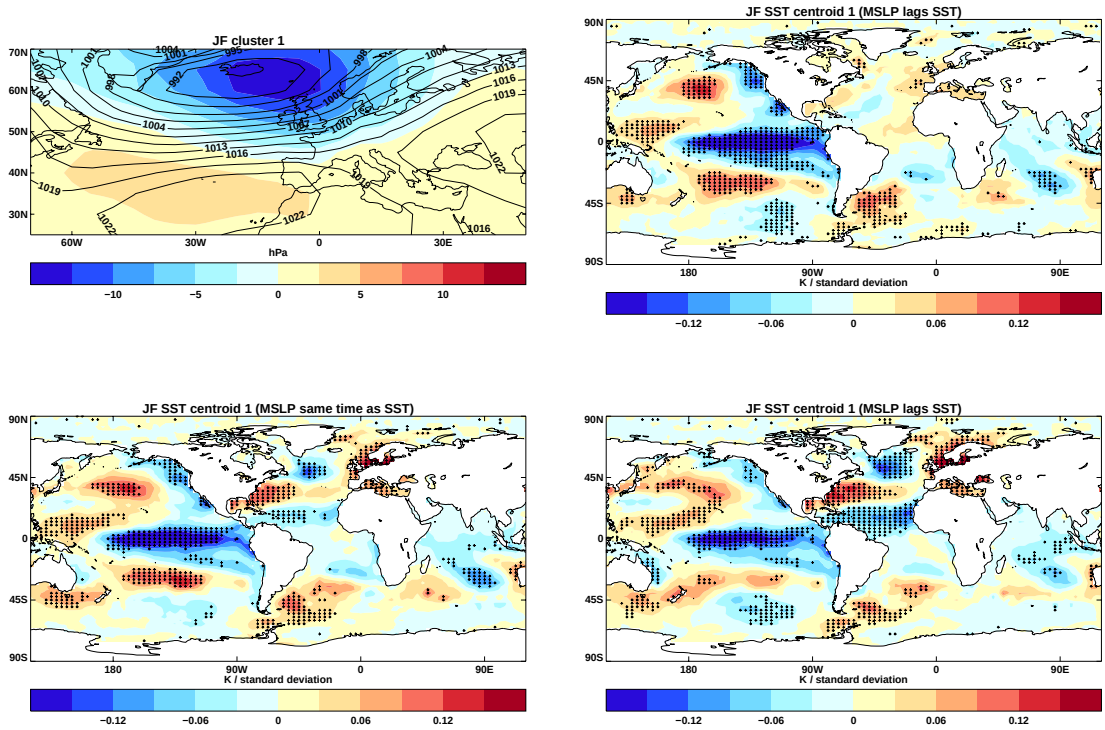


**Figure 3:** Regression of SSTs on the JF cluster 1 (positive phase of NAO) frequency time series for the years 1870-2002. SSTs are shown leading the MSLP by one month, simultaneously with the MSLP and lagging the MSLP by one month. Crosses show grid points significant at the 5% level.

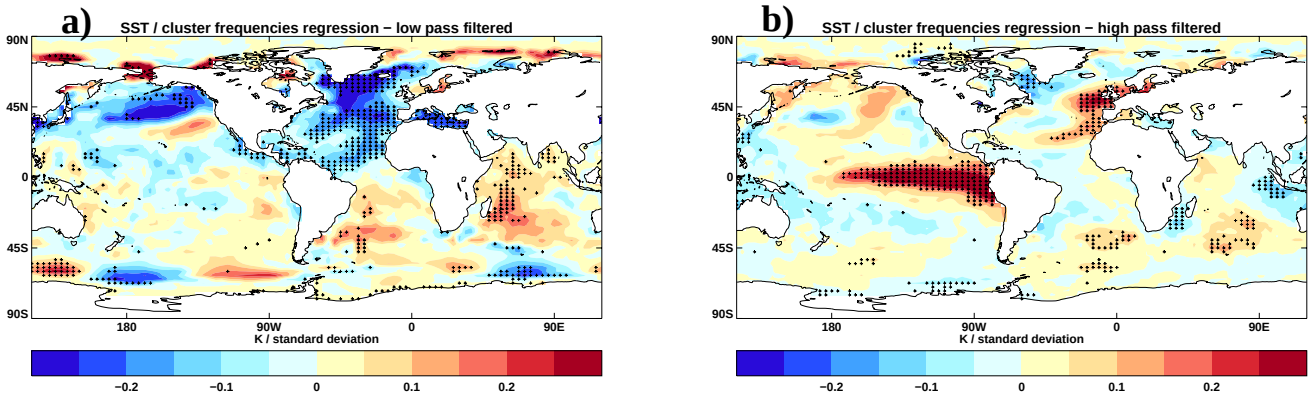


**Figure 4**: Regression of SSTs on the frequency difference time series based on the two JA season clusters associated with the summer NAO a) low pass filtered pattern and b) the high pass filtered pattern (the residual from the low pass filtered pattern) for the years 1950-2002.

The lead-lag relationship between the NAO (defined below) and North Atlantic SST has been further examined using a Granger causality time series modelling approach. Specifically, a Vector AutoRegession (VAR) model was used to examine the feedback process between North Atlantic SST and the NAO. The NAO used here was the first principle component of monthly EMSLP fields (calculated over all months). In this situation a variable X1 (i.e. SST) is causal for another variable X2 (i.e. NAO) if knowledge of the past history of X1 is useful for predicting the future state of X2 over and above the knowledge of the past history of X2 itself (see Mosedale *et al*. [2006]; Granger [1969]). Significance can be tested with the Omega statistic.

The Omega statistic p-value of North Atlantic SSTs influence on the NAO is plotted in Figure 5a. Areas in red are highly significant, indicating that SST in these areas influence the NAO up to 6 months prior to the current NAO. This pattern of significant influence reveals the well known North Atlantic tripole SST pattern (seen also in Figure 3). The reverse situation can also be considered (Figure 5b), highlighting regions where prior values of the NAO can have a significant influence on North Atlantic SST.

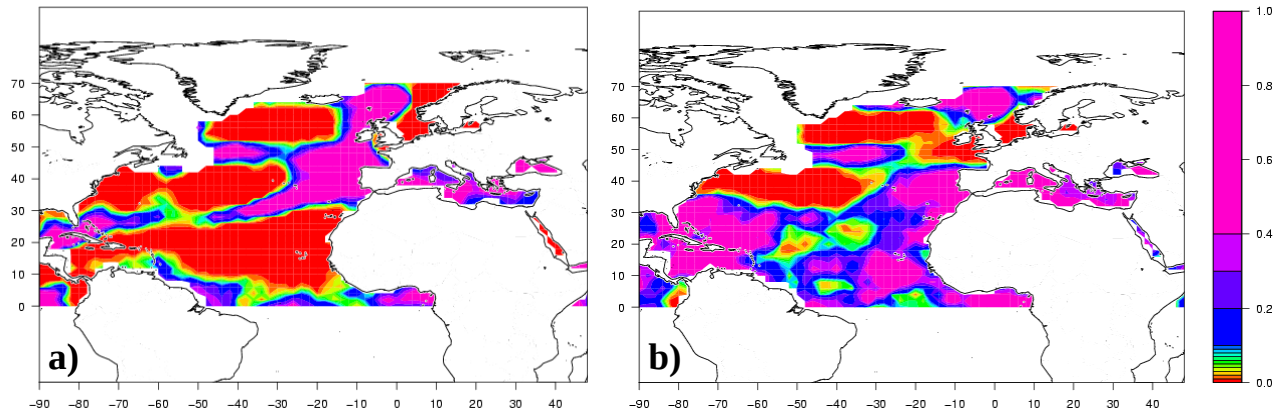


**Figure 5: a)** Lagged SST (up to six months) influence on the NAO calculated over all months for 1880-2003. Shown is the p-value of the Omega statistic Granger causality test. **b)** Lagged NAO (up to six months) influence on SST calculated over all months for 1880-2003. Shown is the p-value of the Omega statistic Granger causality test. Scale for figures is given on RHS.

The relationships between temperature and precipitation with the seasonal cluster patterns will be examined in detail below. We briefly discuss here the influence of North Atlantic SST on the occurrence of temperature extremes (using Bern, Switzerland, and Central England Temperature (CET) 90$^{th}$ percentile maximum temperature indices tx90), again using the Granger causality approach. The VAR models show that extreme temperatures in these two different locations in Europe show different areas of potential predictability from North Atlantic SSTs. For CET tx90, a large area of SST around the British Isles, extending south- and west-ward into the Azores region is where we can expect some predictability of extreme temperature. For Bern tx90, temperatures in the Mediterranean as well as SSTs in the central north Atlantic east of the Iberian Peninsula appear to have some influence. Della-Marta *et al.* [2006] found a similar SST pattern to those in Figures 6 a, b from a canonical correlation analysis, using SST to predict extreme summer temperatures over Western Europe.

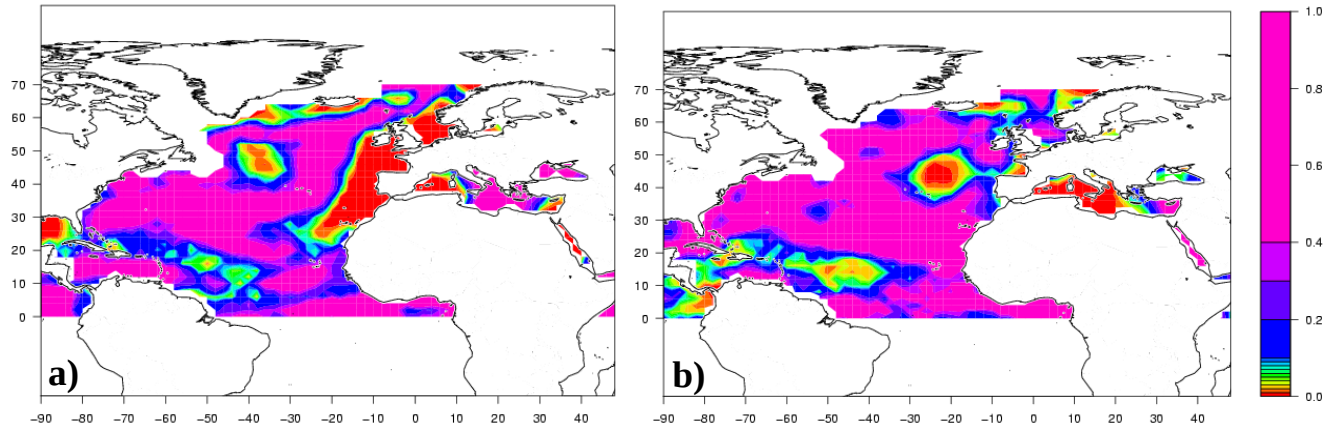


**Figure 6:** Lagged SST (up to three months) influence on the a) CET tx90 series and b) Bern tx90 series calculated over all months together for 1880-2003. Shown is the p-value of the Omega statistic Granger causality test. Scale for figures is given on RHS. SST areas significantly affecting Tx90 at the 5% level are in yellow and red.

## 4) Relationships between cluster patterns with temperature and precipitation

In this section we summarise the observed relationships between European temperature and precipitation with the seasonal cluster patterns. In section 4.1 the relationship is examined over the whole cluster period 1850-2003. In section 4.2 we then consider the time-varying influence of the atmospheric circulation on the temperature and precipitation indices.

### 4.1 Surface temperature anomalies and SLP cluster association

Patterns of co-variation between pressure and surface temperature patterns over the last 150 years are examined, using the seasonal surface pressure cluster patterns and 76 European surface temperature stations from the ECA data base [Klein Tank *et al.*, 2002]. For each cluster pattern or regime (and season), Spearman correlations were computed between the cluster frequencies and the anomalous mean temperature. We note that a number of the SLP clusters are very rare during the 20$^{th}$ century, which leads to very few different values of the cluster frequencies. Results with 'rare' clusters should be viewed with caution.

There is some spatial coherence of the covariation, although the correlations are generally very small and barely significant for MAM, JJA and SON (see Appendix). They are however large in the winter (Figure 7), with clusters 1 (positive phase of NAO) and 5 (Atlantic ridge and Siberian high) (see Figure 1 for DJF cluster patterns) having the highest correlations with temperatures. For each station and season, the 0, 20, 40, 50, 80 and 100$^{th}$ quartiles of temperature anomalies were then determined, classified as 'very cold', 'colder than normal', 'median', 'warmer than normal' and 'very warm'. For each season, station and each quartile of temperature, the number of days spent in each SLP cluster was determined. From this the most probable quintile of temperature for each cluster was chosen, adopting the approach of Yiou and Nogaj [2004]. In all seasons there is an interesting spatial coherence of the cluster/temperature association, with north-south and east-west gradients. This is enhanced for 'very cold' or 'very warm' anomalies. For winter, shown in Figure 8, most clusters are associated with colder conditions, with the exception of cluster 1 (positive NAO) and cluster 3 to the south.

### 4.2 Time-varying influence of the atmospheric circulation on the temperature and precipitation indices

The relationship between the daily MSLP clusters and the temperature and precipitation (based here on daily station time series from WP4) has also been examined for the sub periods used in section 2[1]. All 328 precipitation and 242 temperature records were included in the analysis, despite inhomogeneity problems [Della-Marta & Wanner, 2006]. Anomalies were formed by removing the whole-period mean for each station. Then, for each cluster pattern the precipitation and temperature anomalies for those cluster days were averaged for each station. This analysis was repeated for each sub period. There was a large degree of correspondence between the temperature and rainfall deviations and conditions to that expected from the pressure distributions of the cluster centroids. Due to space restrictions only a subset of all available plots are shown here; see http://phygeo7.geo.uni-augsburg.de/emulate/wp3/ for all plots.

[1] Sub periods are: SP1 = 1850-1900, SP2=1901-1951, SP3=1952-2003. The full period covers 1850-2003.

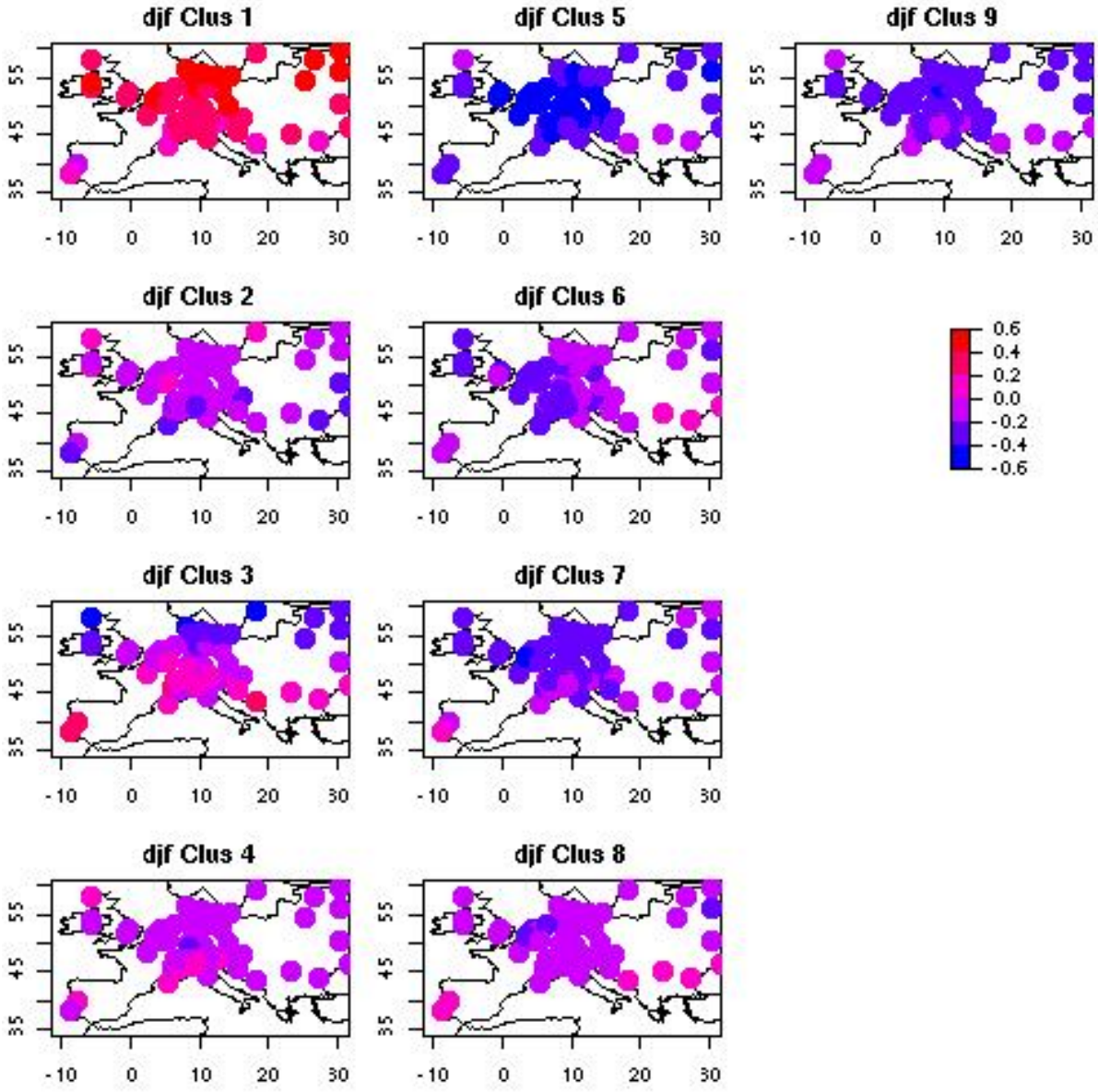


**Figure 7**: Spearman (rank) correlation coefficient between regime frequency and temperature for the Winter (DJF) season. The colour codes indicate the correlations for each station for the common period 1910-2002. All station records begin prior to 1910, but have variable start dates (see Klein Tank *et al.* [2002] for more details).

In Figure 9a anomalously warm temperatures are associated with the winter (DJF) cluster 1 pattern (representing the positive NAO) for the period 1850-2003, consistent with Figure 8. Throughout the sub periods (Figures 9b-d), temperatures change from cool-neutral conditions in 1850-1900 to anomalously warm in 1952-2003. For DJF precipitation, cluster 4 and 5 were the wettest for Central Europe (results for cluster 4 are shown in Figure 10). Conditions over the whole (1850-2003) and last sub periods were wet (Figures 10a, d). For the earlier sub periods 1 and 2 however, parts of Central Europe had more dry– neutral conditions (Figures 10b, c).

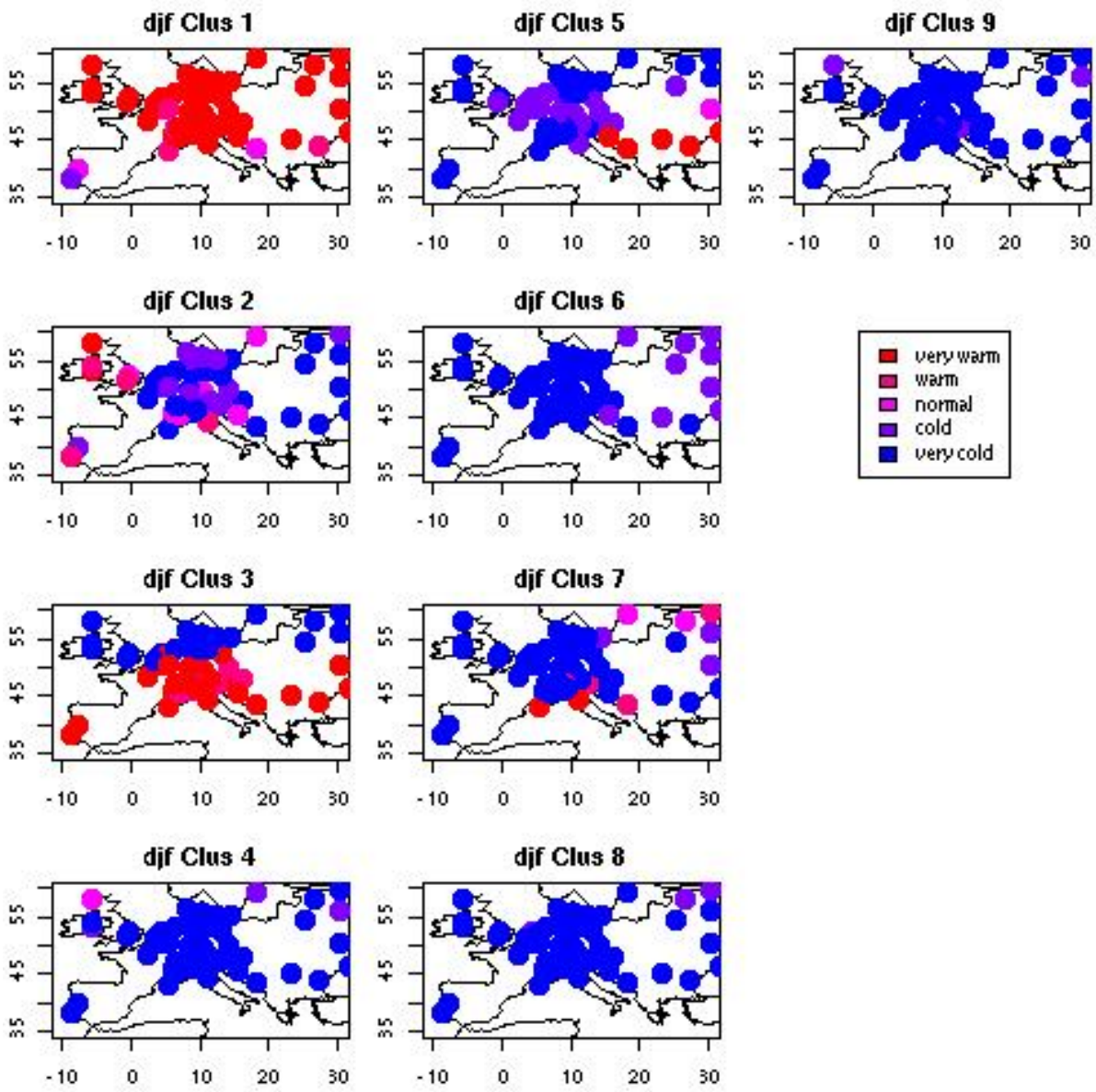


**Figure 8**: Association between SLP clusters and European mean surface temperature (TG) anomalies in the winter (DJF) season. The colour codes indicate the temperature classification for each station over the common period 1910-2002. All station records begin prior to 1910, but have variable start dates (see Klein Tank *et al.* [2002] for more details).

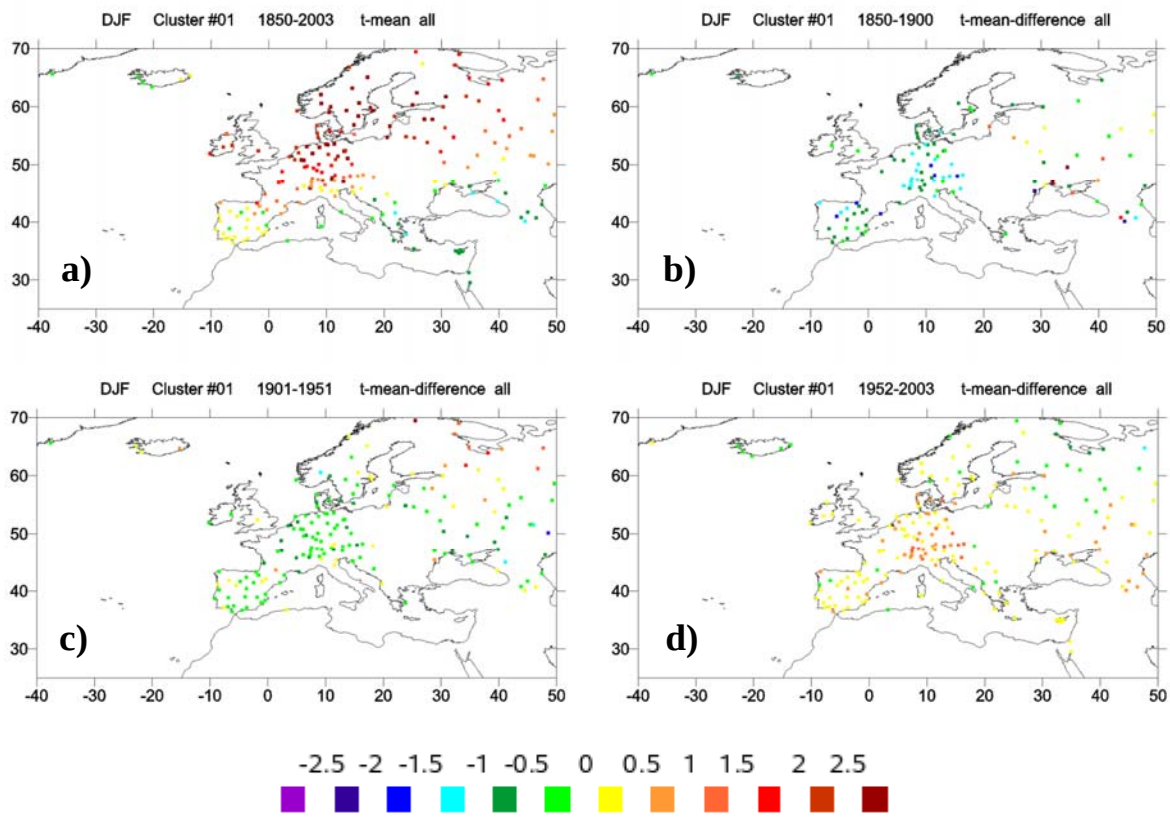


**Figure 9:** Temperature anomalies based on EMULATE station time-series within a) 1850-2003 b) 1850-1900, c) 1901-1951 and d) 1952-2003 for whole-period-EMSLP-cluster 1 for winter (DJF). Plots of all clusters are found at: http://phygeo7.geo.uni-augsburg.de/emulate/wp3/

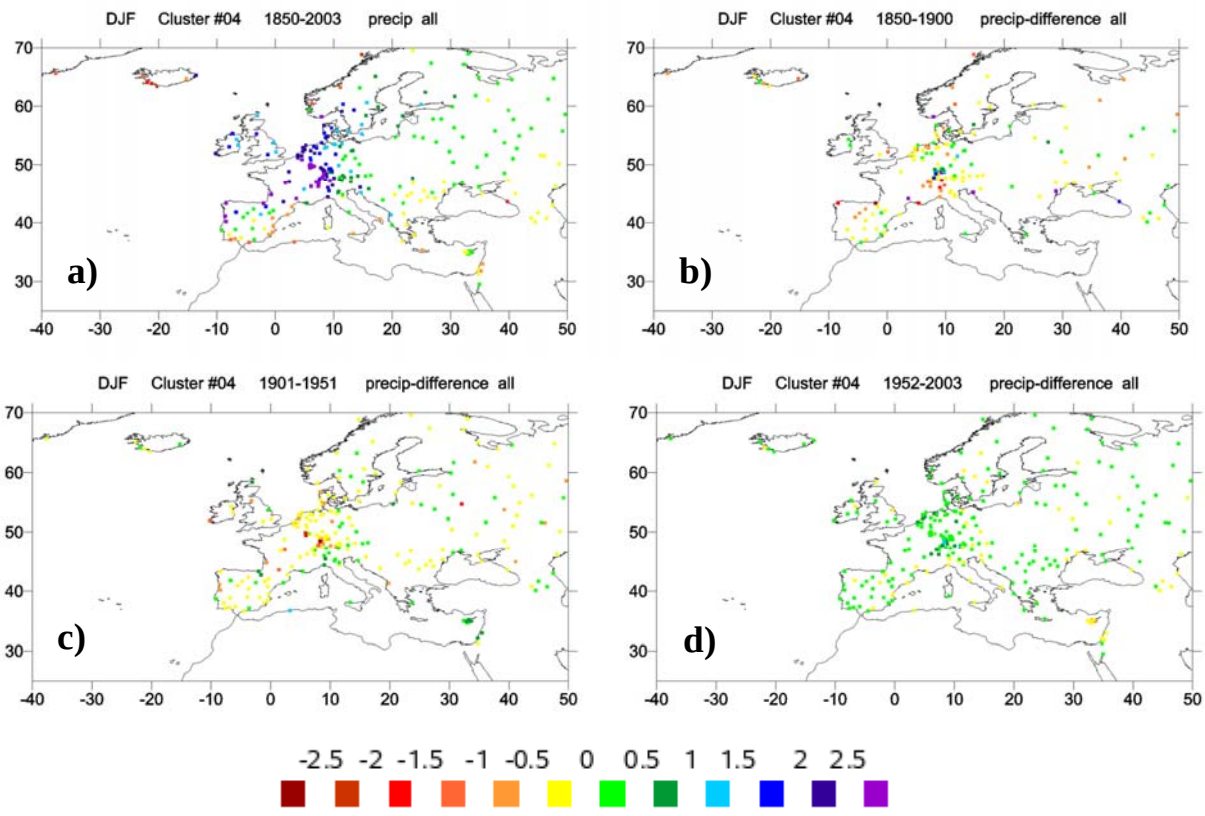


**Figure 10:** precipitation anomalies based on EMULATE station time-series for whole-period-EMSLP-cluster 4 for winter (DJF), within a) 1850-2003 b) 1850-1900, c) 1901-1951 and d) 1952-2003. Plots of all clusters are found at: http://phygeo7.geo.uni-augsburg.de/emulate/wp3/

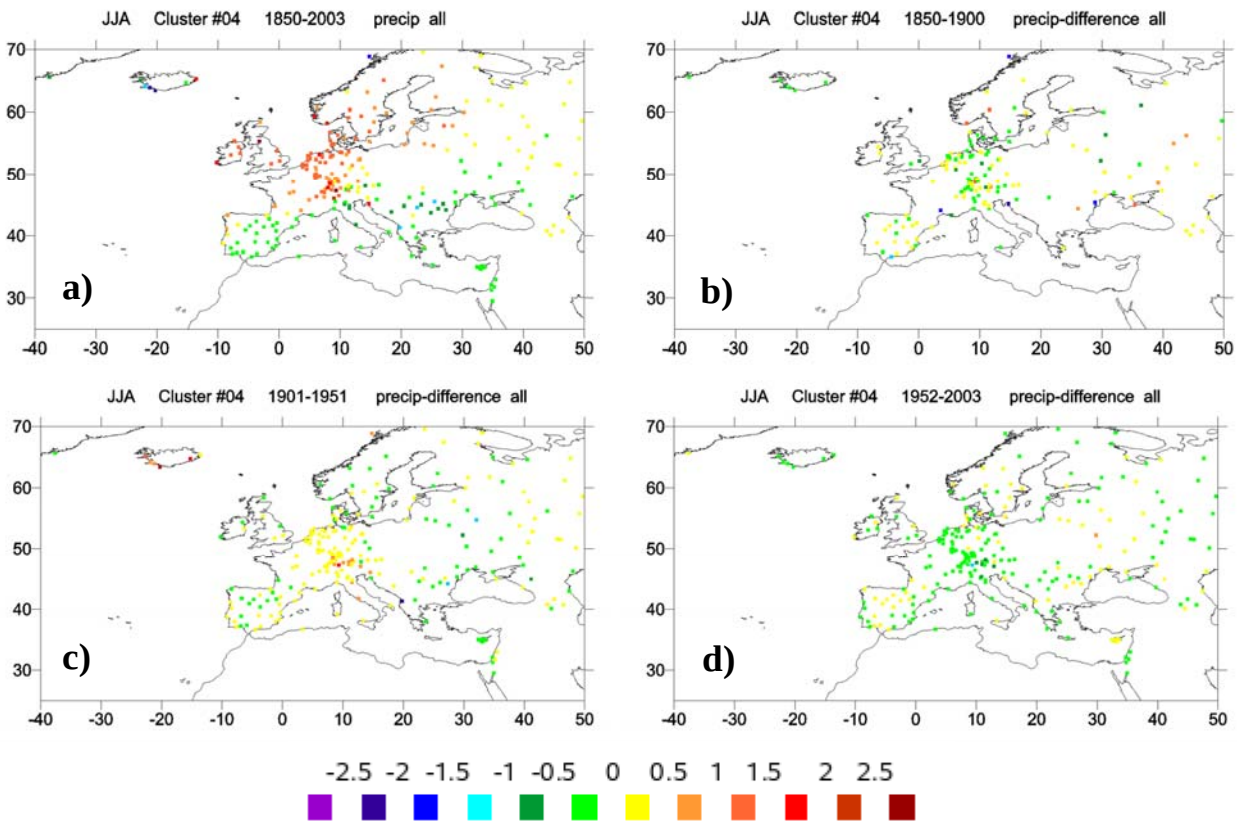


**Figure 11:** Temperature anomalies based on EMULATE station time-series for whole-period-EMSLP-cluster 4 for summer (JJA) within a) 1850-2003 b) 1850-1900, c) 1901-1951 and d) 1952-2003. Plots of all clusters are found at: http://phygeo7.geo.uni-augsburg.de/emulate/wp3/

In summer, clusters 1 and 2 can be characterised as having continuously warm conditions. Cluster 4 (positive mode of summer NAO[2]) had the driest conditions, shown in Figure 11 and a longer-term positive trend in seasonal cluster frequency (much as described in report D7 for the JA summer NAO). For autumn, cluster 6, the wettest in autumn, continues to become wetter. This cluster is also associated with warming from 1901-1951 to 1952-2003. Clusters 7 and 8 are associated with strong warming, with the former becoming much drier in central Europe.

Mohammad *et al.* [2006] focused specifically on the time-varying influence of the NAO on 25 of the WP4 temperature and precipitation indices over north-western Europe and Iberian Peninsula. Seasonal 31-year running mean correlations over the period 1916-1985 were calculated between the NAO (derived from a seasonal EOF analysis of daily EMSLP fields i.e. the NAO is defined separately for each 3 month season). For most indices, the time variations were small and insignificant; however there are some interesting changes over the 20th century. Results from 4 indices are presented in figure 12. The correlation for winter mean daily temperature over north-western Europe and the NAO is high over the 20th century, though dips slightly around 1920. For the winter 98th percentile temperatures, the correlations are very poor in the first half of the 20th century, but gradually rise and then remain constant around 0.5 from the 1960s. Interestingly the spread between the individual station records increases from the 1960s. The mean winter precipitation total correlations are generally poor, though there is an indication of stronger correlations with some individual stations (green curve). There are also considerable interannual-decadal fluctuations in the correlations. In contrast, the summer precipitation total correlations are generally strong and have been increasing since the

[2] NOTE, the summer NAO is most commonly defined for the months July and August, rather than June, July, August presented here.

1960s. There is large spread amongst the individual station correlations, particularly with precipitation.

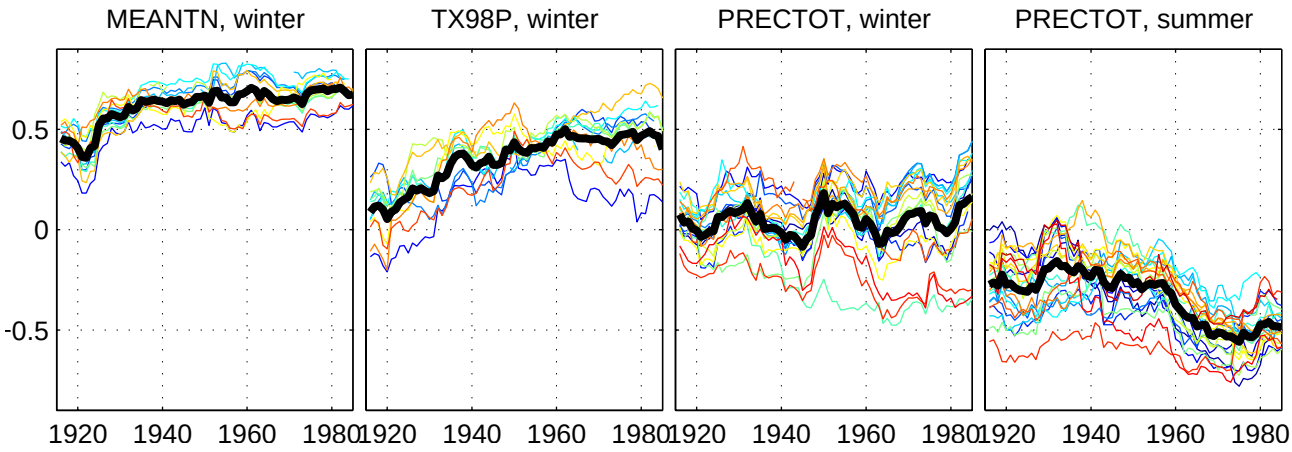


**Figure 12**: The time evolution of the correlations between the NAO and regional mean winter daily temperature (MEANTN), 98$^{th}$ percentile of daily maximum temperature (TX98P), winter sum of daily precipitation (PRECTOT) and summer sum of daily precipitation (PRECTOT) for stations in north-western Europe, calculated in a running 31-year window for selected indices. This yields correlation data for the period 1916-1985. The thin coloured lines represent the correlations for each individual station in the region and the heavy black line is their average.

## 5. European Droughts

Here we analyse the database of drought index for Europe, developed as part of D8 and document the influence of circulation types on drought over Europe. Trends in moisture availability over Europe are also analysed.

Maps of monthly self-calibrating Palmer Drought Severity Index (scPDSI) have been calculated for the period 1901-2002 for Europe as a whole (35-70°N and 10W-60°E) with a spatial resolution of 0.5° x 0.5°. As reported in van der Schrier *et al.* [2006], there is a lot of decadal scale variability over the region as a whole. The mid-1940s to early 1950s stand out as a persistent and exceptionally dry period, whereas the mid-1910s and late 1970s to early 1980s were very wet (Figure 13). The driest and wettest summers on record, in terms of the amplitude of the index average over Europe, were 1947 and 1915 respectively, while the years 1921 and 1981 saw over 11% and 7% of Europe suffering from extreme drought or wet conditions respectively.

Trends in summer moisture availability over Europe for the 1901-2002 period fail to be statistically significant, both in terms of spatial means of the drought index and in the area affected by drought. In Figure 14 the trends over the period 1950-2002 are presented. These results do not support the findings of Dai *et al.* [2004] of widespread and unusual drying over European regions as a whole over the last few decades.

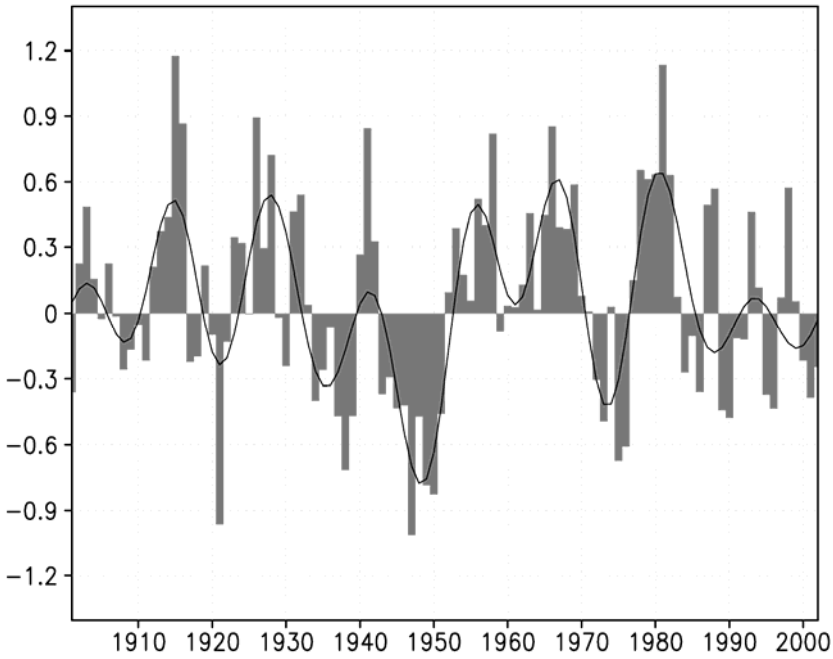


**Figure 13:** Mean European summer scPDSI. The values are a spatial average of all grid boxes, weighted with the cosine of the latitude. The solid line shows the 10-year low-pass filtered values. The three driest and wettest years on record are 1947, 1921, 1950 and 1915, 1981, 1926, respectively. Figure is taken from van der Schrier *et al.* [2006].

Using the scPDSI database, we consider links between circulation patterns and summer soil-moisture status. The summer soil-moisture status represents the integration of the weather conditions of the preceding winter and spring and the 'current' summer. The aim was to determine how much of the summer soil-moisture status, can be explained by winter and spring circulation fields.

Characteristic summer soil-moisture patterns have been identified (using Empirical Orthogonal Teleconnection patterns); the first six of these (Table 1) have been used for correlating with the different circulation index series (Euclidian distance indices and correlation indices [after Philipp *et al.*, 2006]) for the preceding winter and spring seasons and the current summer. The period examined was 1901-2002.

It was found that summer soil moisture status (as measured by the scPDSI, van der Schrier *et al*., [2006]) shows reasonable degrees of predictability using indices of antecedent behaviour of atmospheric circulation, for some typical patterns of scPDSI. Correlations between circulation indices for specific seasons and the intensity of individual soil-moisture patterns range from 0 to 0.4. When the strongest circulation predictors were grouped (for individual seasons) and multiple regression was performed, multiple correlation co-efficients as high as 0.56 were achieved. Strong relationships were obtained with region III (North West Europe near and including south east UK).

| PDSI pattern | Principal centres of drought for each pattern |
|---|---|
| I | North of the Caspian Sea (*ca.* 50° N, 50 ° E) |
| II | West of the Black Sea (*ca.* 45°N, 20° E) |
| III | SE UK and adjacent areas to the E and SE ( *ca.*50° N, 5°E) |
| IV | West of the Caspian Sea (*ca.* 42° N, 55°E) |
| V | North western Russia (*ca.* 57°N, 40° E) |
| V1 | South western France (*ca.* 43°N, 3° E) |

**Table 1:** The six scPDSI patterns and their principal region of associated drought effect.

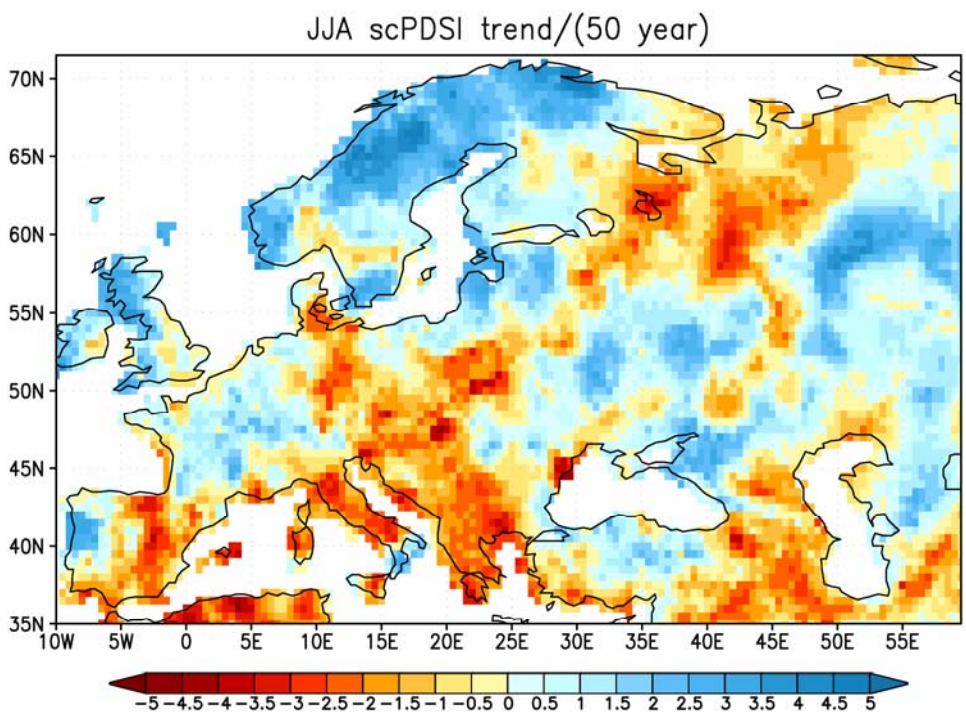


**Figure 14:** Trends per 50 years in the scPDSI calculated over the period 1950-2002. Note that no information is given on the statistical significance of these trends. Figure is taken from van der Schrier *et al.* [2006].

## 6. Interannual Relationships with ENSO

### 6.1 Winter

Composite analysis of cluster frequencies based on years with weak or strong ENSO events were examined and revealed a different response for weak events compared to strong events. The results for JF and MA are presented in Figure 15. The solid line represents confidence intervals[3] for strong ENSO years (1877,1888,1899,1930,1982,1997) and the dotted lines are confidence intervals for weak ENSO years (1896, 1902, 1905, 1911, 1918, 1925, 1939,1941,1957,1965,1972,1991). Here the ENSO year is defined as the first year of the ENSO event. Black represents observations and green represents the long (1870-2002) all forcings model runs; we consider only the observations here. For each cluster, the average cluster frequency in the years *following* the ENSO year enumerated above is calculated, represented by the crosses on the plot. For JF, such years are usually at the peak of the ENSO listed as starting in the previous year.

For JF after a strong ENSO event (often the actual peak of an event straddling two years), there is a reduced frequency of cluster 7 (Figure 15a). By contrast there are an above average number of cluster 7 events after a weak ENSO event. A similar result is found with cluster 6, though the response after the strong ENSO response is within the confidence limits. The opposite occurs for clusters 2, 4 and 6, with a large response after strong ENSO events and a weak response after weak events. Such a highly non-linear response in winter is qualitatively consistent with an analysis of the non linearity of ENSO influences on North Atlantic/European atmospheric circulation made by Toniazzo and Scaife (see report D12) using a climate model. For MA (Figure 15b), after weak ENSO events there a below average number of cluster 5 events, whereas after strong ENSO events, there is a below average number of cluster 9 events.

[3] The confidence intervals are 90% and are generated by averaging the cluster frequencies for 10000 random groups of years (where the number of years in each average 12 for the weak ENSO years and 6 for the strong ENSO years).

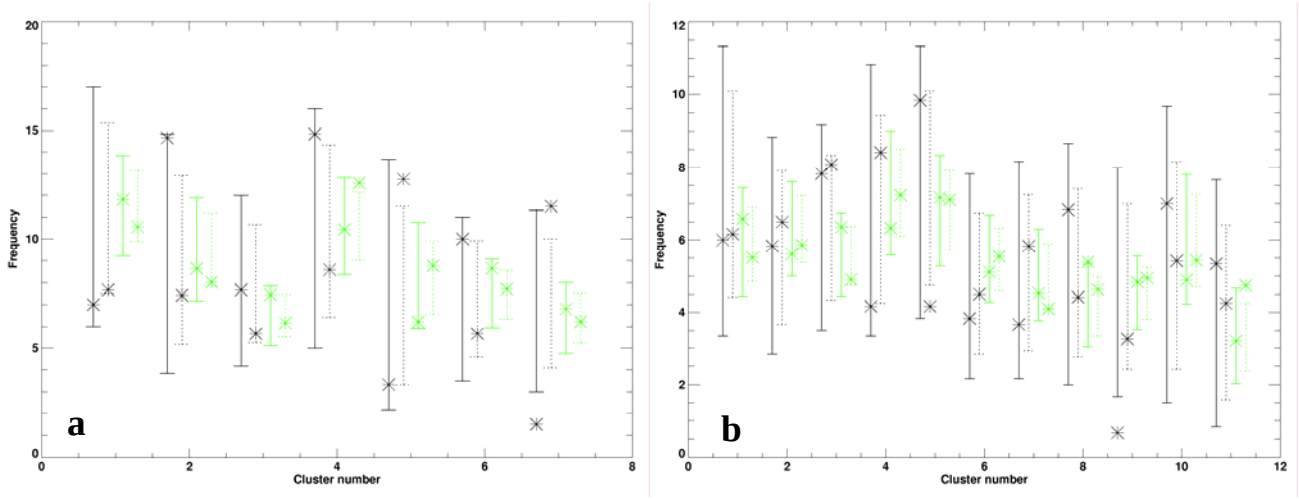


**Figure 15**: Cluster frequencies associated with strong (black solid line) and weak (black dashed line) ENSO events (model results are also shown in green, but not discussed here) for a) JF and b) MA. See text for weak/strong ENSO years.

### 6.2 High summer.

Figure 4b showed some evidence of the influence of ENSO on the summer North Atlantic Oscillation (SNAO). This is emphasised further in Figure 16a, the squared coherency between the positive (anticyclonic over UK) phase of the SNAO and Nino 3.4 SST over the long period 1876-2003. On ENSO time scales near 3-4 years the squared coherency is highly significant at well beyond the 5% significance level (for this particular smoothing of the spectra and data length, this is near 0.45). Figure 4b shows the link is with the El Nino phase. A similar analysis for the negative phase shows a coherence near 0.5 which is still significant, suggesting a weaker link with La Nina.

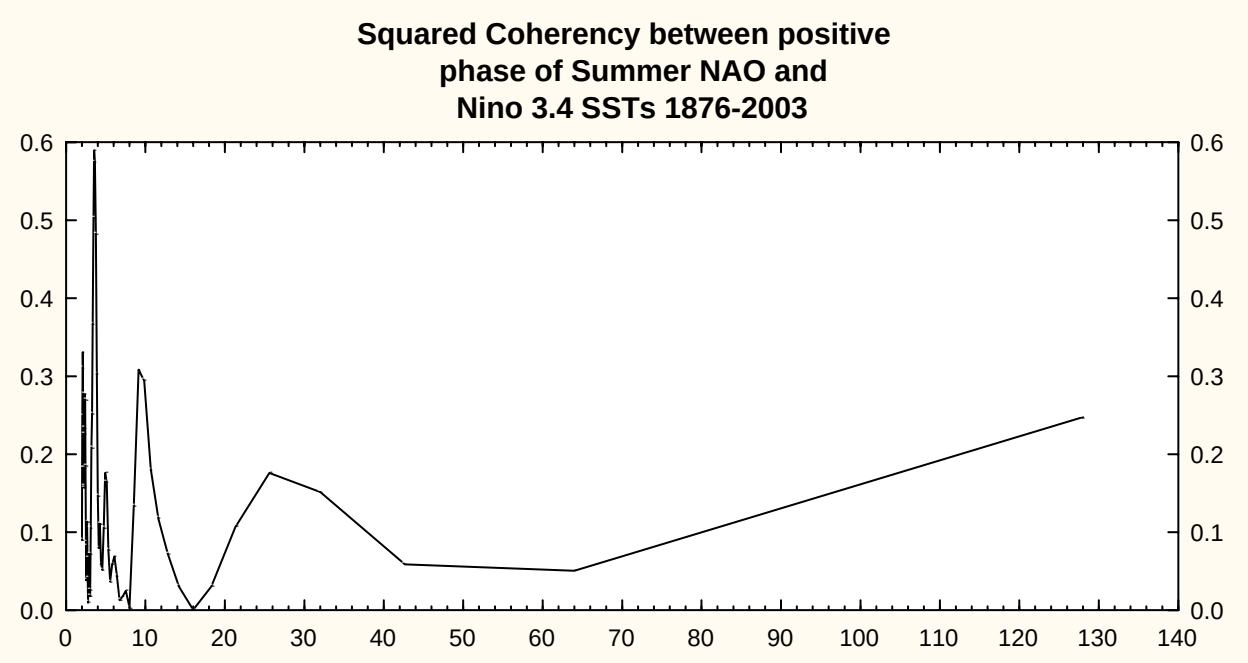


**Figure 16a:** Squared coherence between the positive phase of the Summer North Atlantic Oscillation, as measured by the first EOF of pressure at mean sea level in July and August of daily EMSLP data over the period 1881-2003, and Nino 3.4 SST for 1876-2003 as derived from HadISST.

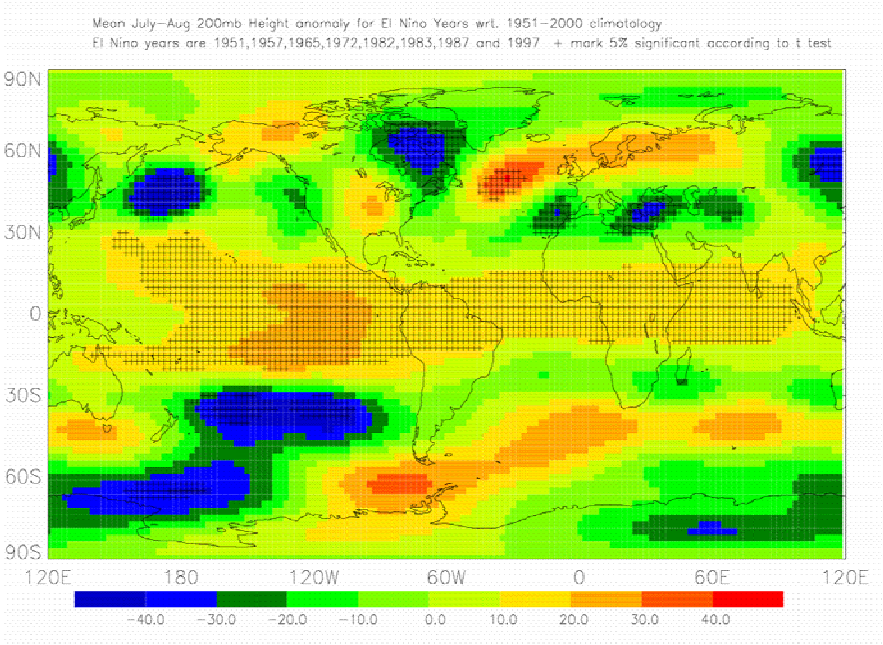


**Figure 16b:** Mean July and August 200hPa height anomalies, relative to a 1951-2000 climatology, during the eight strongest El Niños over this period, as measured during July and August in the Nino 3.4 region of the tropical Pacific. A signature of the positive phase of the summer NAO can be seen over the Greenland-European region.

Further confirmation comes from a superposed epoch analysis of 200hPa height (and lower levels) over the period of the NCEP Reanalysis and the 8 strongest El Niños as measured in high northern summer. (The Summer NAO appears to be nearly equivalent barotropic in character). A clear signature of the positive phase of the SNAO emerges, with locally significant centres over Greenland and the North Atlantic to the south west of UK.

The question then arises as to how such a link could occur in summer. Fig 16b suggests that a Rossby wave like response that may emanate from the north West Pacific. A series of idealised SST experiments is being run with HadGEM1 to test the hypothesis that much of the ENSO forcing actually comes from the Tropical West Pacific warm pool. This reaches its furthest north position in July and August. During El Nino, the tropical West Pacific actually cools in such a way that the SST gradient from south to north increases. This may set up more convergence into the north of the warm pool and hence increased precipitation there and anomalous diabatic forcing near 20N. There is thus the potential to interact with the sub tropical jet stream just to the north. Additional effects may arise from the equatorial Pacific itself where rainfall increases substantially near the date line. However, there is a theoretical problem with communicating diabatic forcing near the equator with the northern extratropics in northern summer. Results from such work are beyond the period of the EMULATE project

## 7. Atmospheric circulation and the Ratcliffe and Murray (RM) North Atlantic SST pattern in winter

Ratcliffe and Murray [1970] and Palmer and Sun [1985] among others have shown that SST variations east of Newfoundland vary strongly in late autumn and early winter and can force the atmosphere in a Rossby wave like barotropic response (Fig 17). A warm RM SST anomaly is associated with a northward deviation of the storm track in the western North Atlantic and a cold anomaly with a more southerly track, especially in early winter [Palmer and Sun 1985, Lau and Nath, 1990]. The

warm anomaly is also associated with blocking over high latitudes of north west Russia while a cold RM anomaly tends to be associated with blocking over Iceland to Scandinavia. More recently, it has been realised that the westerly (positive) and easterly (negative) phases of the NAO are forced to some extent in winter by a tripole SST pattern covering the whole north Atlantic as described above (e.g. Rodwell *et al*, 1999). The Ratcliffe SST pattern is superimposed on the more extensive tripole SST pattern; the combined influences of the two SST patterns have not been investigated. In addition the North Atlantic as a whole is warm, thought in part to be due to a warm North Atlantic phase of the thermohaline circulation or Atlantic Multidecadal Oscillation (Knight *et al*, 2005), as well as global warming.

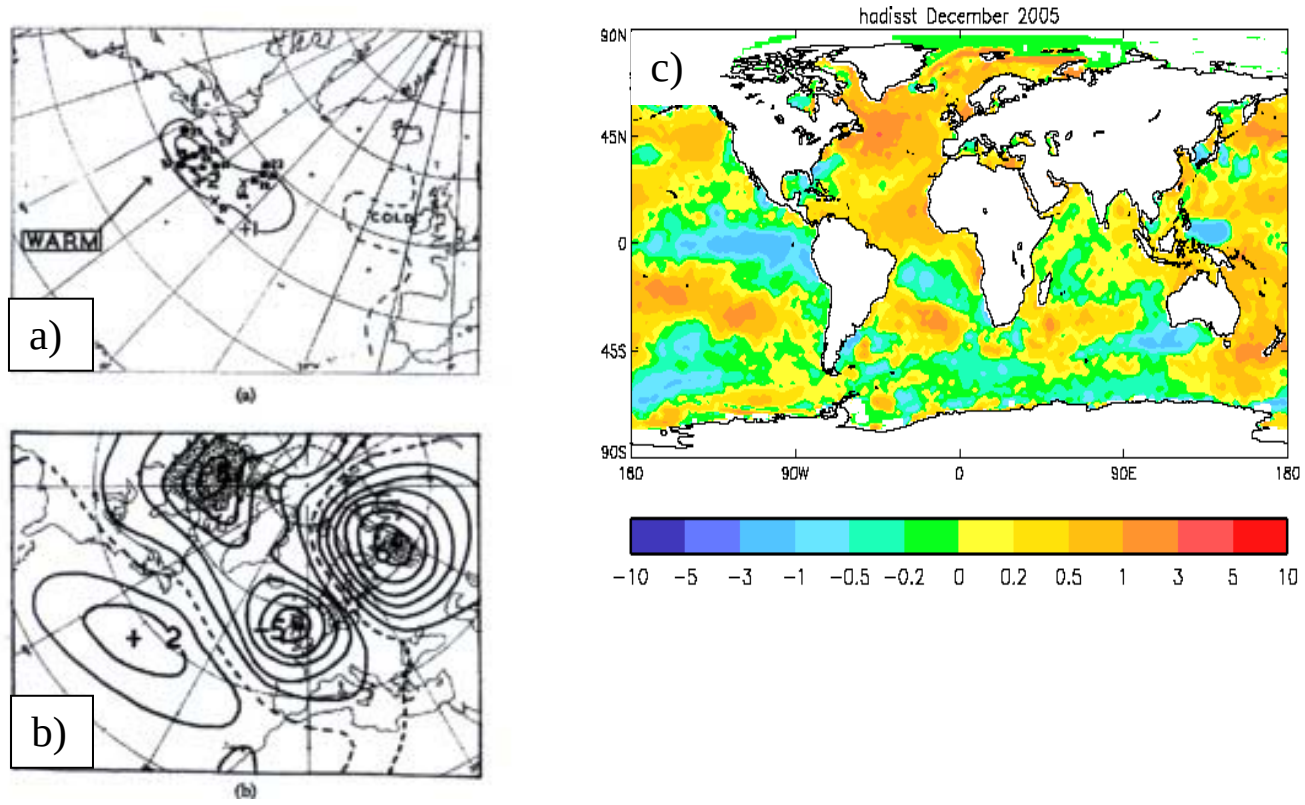


**Figure 17:** Observed relationship between warm SST east of Newfoundland in December (a) and anomalies of December pressure at mean sea level (b) found by Ratcliffe and Murray [1970]. c) Global SST anomalies from a 1961-90 base climatology during January 2006 taken from the HadISST data set [Rayner *et al*, 2003]. A very warm RM region with a central anomaly value of 3°C can be seen.

An excellent test bed may be the winter of 2005-6. Here a very strong negative phase of the SST tripole (favouring a strong negative NAO and blocking over Iceland-Scandinavia) was associated with an extremely strong warm RM SST anomaly (having a persistent winter centre with a near 3°C magnitude, favouring a strengthened storm track north of Iceland extending downstream over the North Sea - west Scandinavian region). The issued and generally successful Met Office winter temperature forecast for Europe in 2005-6 (see Part 6, Final Project Report) was heavily reliant on the strong negative SST tripole, but largely neglected any additional influences of Ratcliffe area SST forcing. In winter 2005-6 the expected blocking over Iceland was lacking until fairly strong blocking developed February, but blocking over north east Scandinavia and north west Russia was very pronounced.

Although beyond the EMULATE research period, experiments are underway with the HadGEM1 climate model to investigate the joint effect of these observed SST anomalies on the atmospheric circulation in winter 2005-6. The experiments are designed take account of new insights that suggest that the stratosphere may quite often play a strong feedback role in winter NAO responses to SST forcing [Scaife *et al*, 2005].

## 8. Concluding remarks

We have reported some of the effects of SST on precipitation and temperature in Europe and on the main direct influence on both, by regional atmospheric circulation. The latter has been measured through both cluster and empirical orthogonal function analysis. In winter the North Atlantic Oscillation clearly shows up in cluster analyses and the NAO cluster is, as expected, associated with a tripole SST pattern over the North Atlantic. More than one method of analyses shows this clearly. Both SST and the winter NAO influence each other, with a stronger influence of the NAO on SST than vice versa, at least interannually. In summer, the summer North Atlantic Oscillation (SNAO) atmospheric cluster or empirical orthogonal function discussed in report D7 is clearly associated with SST. Interdecadally the SNAO is associated with the Atlantic Multidecadal Oscillation in SST and El Nino interannually. These results mirror model results in D12, though the observed interannual relationship of the SNAO with ENSO seems stronger than that modelled. There is some evidence that the observed El Nino effect on the SNAO may be stronger than the observed La Nina effect.

The association between the clusters as defined in EMULATE and surface temperature outside winter is rather weak over Europe. In winter the cluster associated with positive phase of the NAO is associated mainly with warm conditions over central and northern Europe, as expected. The relationship is strong. Such conditions are therefore associated with the positive phase of the SST tripole over the North Atlantic. Most other winter clusters are associated with cold to near normal conditions. Associations with SST for these clusters have yet to be assessed. There is some evidence for time-varying influences of the NAO on European temperature and rainfall. Any causes related to SST have yet to be investigated. There are no trends in Europe wide drought. However the more regional influence of the SNAO on drought e.g. as measured by the scPDSI, needs investigation as the phase and strength of the SNAO clearly influences north west European rainfall. Finally, we note that the additional influence in winter, especially early winter, of the quite frequent warm or cold SST regions east of Newfoundland (the Ratcliffe and Murray region) compared to the SST tripole in winter is of interest. This is particularly so in the context of the 2006 cold European winter when the early winter (December) Ratcliffe and Murray SST anomaly reached an extreme 3°C. The European winter of 2006 and SST influences are currently under investigation and will be reported elsewhere.

## References


Ansell, T., Jones, P.D., Allan, R.J., Lister, D., Parker D.E., Brunet-India, M., Moberg, A., Jacobeit, J., Brohan, P., Rayner, N., Aguilar, E., Alexandersson, H., Barriendos, M., Brazdil, R., Brandsma, T., Cox, N., Drebs, A., Founda, D., Gerstengarbe, F., Hickey, K., Jonsson, T., Luterbacher, J., Nordli, O., Oesterle, H., Rodwell, M., Saladie, O., Sigro, J., Slonosky, V., Srnec, L., Suarez, A., Tuomenvirta, H., Wang, X., Wanner, H., Werner, P., Wheeler, D., Xoplaki, E., 2006: Daily mean sea level pressure reconstructions for the European - North Atlantic region for the period 1850-2003. *J. Climate* (In press).

Cassou, C., Terray, L., Hurrell, J., Deser, C. 2004: North Atlantic winter climate regimes: spatial asymmetry, stationarity with time, and oceanic forcing. *J. Climate*, **17**, 1055-1068.

Dai, A., Trenberth, K. E., Qian, T. 2004: A global dataset of Palmer Drought Severity Index for 1870-2002: Relationships with Soil Moisture and Effects of Surface Warming, *J. Hydrometeorol.*, **5**, 1117-1130.

Della-Marta, P. M., Luterbacher, J., von Weissenfluh, H., Xoplaki, E., Brunet, M., Wanner, H. 2003; Summer heat waves over western Europe 1880-2003, their change and relationship to large scale forcings, *Climate Dynamics*, submitted

Della-Marta, P. M. and Wanner, H. 2006: A method for homogenising the extremes and mean of daily temperature measurements, *J. of Climate*, accepted.

Fereday, D. R., Knight, J.R, Scaife, A.A., Folland, C.K. and Philipp, A. 2006: Cluster analysis of North Atlantic / European weather types, in preparation.

Folland, C.K., 2005: Assessing bias corrections in historical sea surface temperature using a climate model. *Int. J. Climatol.*. (Special issue, CLIMAR II Conference), **25**, 895 - 911.

Granger, C.W.J. 1969: Investigating causal relations by econometric models and cross-spectral methods, *Econometrica*, **37**, 424-438

Hurrell, J.W. and Folland, C. K., 2002: The relationship between tropical Atlantic rainfall and the summer circulation over the North Atlantic, *CLIVAR exchanges*, **25**, 52-54.

Klein Tank, A.M.G. and Coauthors, 2002. Daily dataset of 20th-century surface air temperature and precipitation series for the European Climate Assessment. *Int. J. of Climatol.*, **22**, 1441-1453.

Knight, J., Allan, R., Folland, C., Vellinga, M., Mann, M. 2005: A signature of persistent natural thermohaline circulation cycles in observed climate, *Geophys. Res. Lett.* **32**, L20708, doi: 1029/2005GL024233.

Lau, N-C. and K.J. Nath, 1990: A general circulation model study of the atmospheric response to extratropical SST anomalies observed in 1950-79. *J. Climate,* **3**, 965-989.

Mohammad, R., Moberg, A., Ansell, T. J. 2006: Correlations between indices for temperature and precipitation extremes in Europe and the leading atmospheric circulation mode during 1901-2000, in preparation.

Moron, G. and Plaut, V. 2003: The impact of El Nino-Southern Oscillation upon weather regimes over Europe and the North Atlantic during boreal winter, *Int. J. Climatol.*, **23**, 363-379.

Mosedale, T. J., Stephenson, D.B., Collins, M., Mills, T. C. 2005: Granger causality of coupled climate process: Ocean Feedback on the North Atlantic Oscillation, *J. of Climate*, accepted.

Palmer, T. and Sun, Z. 1985: A modelling and observational study of the relationship between sea-surface temperature in the Northwest Atlantic and the atmospheric general circulation. *Quart. J. Roy. Meteor. Soc.*, **111**, 947-975.

Philipp, A., Della-Marta, P. M., Jacobeit, J., Fereday, D.R., Jones, P. D., Moberg, A., Wanner, H. 2006: Long term variability of daily North Atlantic- European pressure patterns since 1850 classified by simulated annealing clustering, *J. of Climate*, submitted.

Ratcliffe, R.A.S. and Murray, R. 1970: New lag associations between North Atlantic sea temperatures and European pressure applied to long-range forecasting. *Quart. J. Roy. Meteor. Soc.*, **96**, 226-246.

Rayner, N. A., Parker, D. E., Horton, E. B., Folland, C. K., Alexander, L. V., Rowell, D. P., Kent, E. C., Kaplan, A., 2003: Global analyses of sea surface temperature, sea ice, and night marine air temperature since the late nineteenth century, *J. Geophys. Res*. **108**, No. D14, 4407, doi:10.1029/2002JD002670

Rodwell, M., Rowell, D.P. and C.K. Folland, 1999: Oceanic forcing of the wintertime North Atlantic Oscillation and European climate. *Nature*, **398**, 320-323.

Rodwell, M. and Folland, C.K. 2002: Atlantic air-sea interaction and seasonal predictability, *Quart. J. Roy. Meteor. Soc.*, **128**, 1413-1443

Rodwell, M.R. and Folland, C. K. 2003: Atlantic air-sea interaction and model validation. *Annals of Geophysics. Special Issue for results of EU SINTEX project,* **46**, 47-56.

Scaife, A., J. Knight, G. Vallis and C.K. Folland**,** 2005**:** A stratospheric influence on the winter NAO and North Atlantic surface climate. *Geophys. Res. Lett.* **32**, L18715, doi: 10.1029/2005GL023226.

van der Schrier, G., Briffa, K.R., Jones, P.D. and Osborn, T. J. 2006: Summer moisture variability across Europe, *J. of Climate* (in press).

Yiou, P. and Nogaj, M. 2004: Extreme climatic events and weather regimes over the North Atlantic: When and where?, *Geophys. Res. Lett.*, **31**, Art. No. L07202.

## Appendix

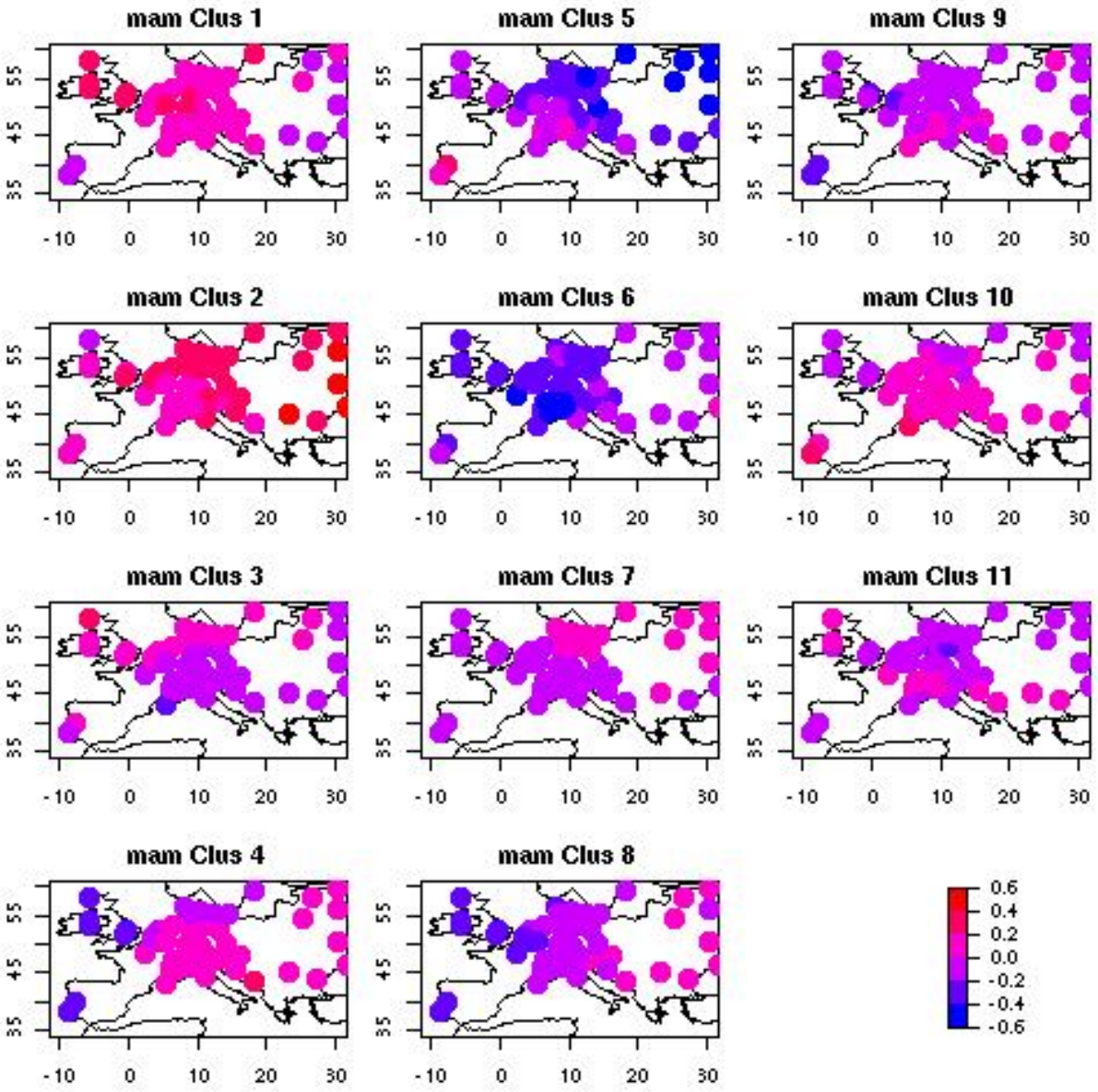


Figure A1: Spearman (rank) correlation coefficients between regime frequency and temperature for the spring (MAM) season. The colour codes indicate the correlations for each station for the common period 1910-2002. All station records begin prior to 1910, but have variable start dates (see Klein Tank *et al.* [2002] for more details).

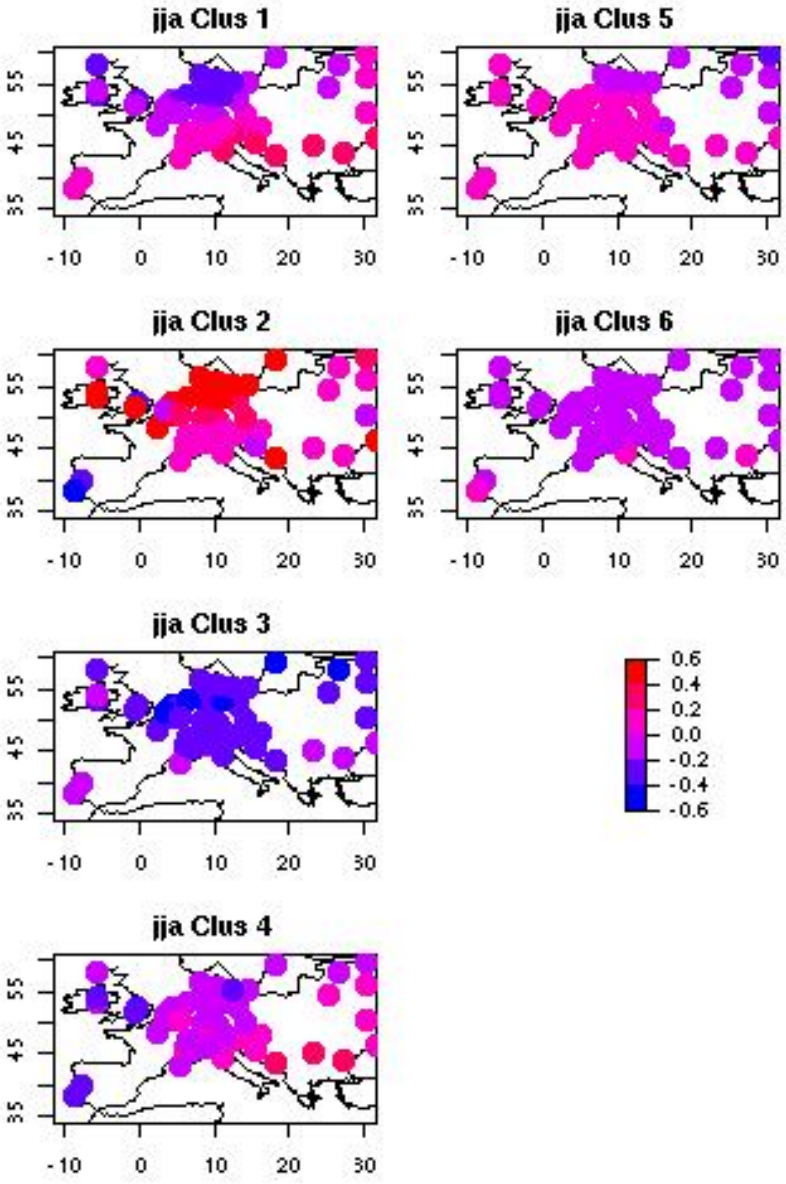


Figure A2: Spearman (rank) correlation coefficients between regime frequency and temperature for the summer (JJA) season. The colour codes indicate the correlations for each station for the common period 1910-2002. All station records begin prior to 1910, but have variable start dates (see Klein Tank *et al.* [2002] for more details).